Accepted Manuscript

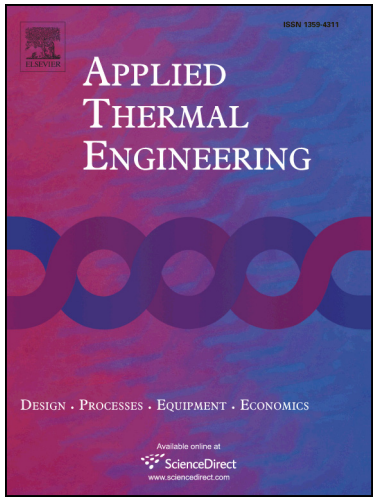

Simulation of the UQ Gatton natural draft dry cooling tower

Xiaoxiao Li, Zhiqiang Guan, Hal Gurgenci, Yuanshen Lu, Suoying He

PII: S1359-4311(16)30333-7
DOI: http://dx.doi.org/10.1016/j.applthermaleng.2016.03.041
Reference: ATE 7909

To appear in: *Applied Thermal Engineering*

Received Date: 23 November 2015
Revised Date: 27 February 2016
Accepted Date: 9 March 2016

Please cite this article as: X. Li, Z. Guan, H. Gurgenci, Y. Lu, S. He, Simulation of the UQ Gatton natural draft dry cooling tower, *Applied Thermal Engineering* (2016), doi: http://dx.doi.org/10.1016/j.applthermaleng.2016.03.041

17th IAHR International Conference on Cooling Tower and Heat Exchanger, 7-11 September 2015, Gold Coast, Queensland, Australia

Simulation of the UQ Gatton natural draft dry cooling tower

Xiaoxiao Li[1] *, Zhiqiang Guan[1], Hal Gurgenci[1], Yuanshen Lu[1], Suoying He[2]

[1] *School of Mechanical and Mining Engineering, The University of Queensland, Brisbane, Australia*
[2]*School of Energy Source and Power Engineering, Shandong University, Jinan, China*

Highlights:

1. The full scale 1-D and 3-D simulation models of a 20m NDDCT was developed.
2. The ambient temperature and hot water inlet temperature effect had been investigated
3. The crosswind effect on the small NDDCT was analysed and discussed

ABSTRACT: A Natural draft dry cooling tower (NDDCT) is a cost-effective cooling technology which can be utilized in most of the small renewable power plants. While a number of numerical studies have been done on NDDCTs in recent decades, experimental studies on full scale small cooling tower are very few. To fill this gap, Queensland Geothermal Energy Centre of Excellence (QGECE) has built a 20 m NDDCT. In this study, a 1-D analytical and a 3-D CFD models of this cooling tower were developed and the cooling performance was investigated at different ambient temperatures, inlet water temperatures and crosswind speeds. The results show that NDDCT in such a size is capable for a 2~3 MW CST power plant. The cooling performance of the NDDCT decreases with the increase in the ambient temperature and the decrease in the inlet water temperature. In terms of the crosswind, the heat rejection ratio decreases with the increase of the crosswind velocity at low crosswind speeds. However, when the crosswind speed becomes large enough, the heat dumped at the bottom of the tower can compensate some losses in cooling capacity caused by crosswind. The results found in the present study give reference for future tests.

Key words: Natural draft dry cooling tower (NDDCT), Cooling performance, CFD modelling

* Corresponding author. *E-mail address:* x.li3@uq.edu.au (X. Li)

Nomenclature

A Area (m^2)
C Inertial resistance factor
C_p Specific heat (J Kg^{-1} K^{-1})
C_D Drag coefficient
d Diameter (m)
h Empirical heat transfer (W m^{-2} K^{-1})
H Height, elevation (m)
K Flow resistance
L length (m)
m Mass flow rate (kg/s)
n Number
P Pressure (Pa)
Q Heat transfer rate (W)
q Heat flux (W m^{-2})
Re Reynolds Number
T Temperature (°C)
v Velocity scalar (m s^{-1})

Greek letters

α Permeability
δ Enthalpy of air (J)
σ Compact area ratio of the heat exchanger
ε Turbulent kinetic energy dissipation (m^2 s^{-3})
η Efficiency
κ Turbulent kinetic energy (m^2 s^{-2})
ρ, Density, mean density (kg m^{-3})
μ Viscosity (kg m^{-1} s^{-1})

Vectors

$\vec{F}$ Force
$\vec{v}$ Velocity
$\hat{i}, \hat{j}, \hat{k}$ Unit vectors of x-, y-, z- direction in Cartesian coordinate system

Subscripts

a, w Air side, water side
cw Crosswind
e Effective
fr front area
he Heat exchanger
i, o Inside or inlet, outside or outlet
t Tube
u Over all
0 Reference value
ts Tower support
ctc Heat exchanger compact
cte Heat exchanger expansion
cto Tower outlet
1,2,3,4,5 Different location of cooling tower

1. INTRODUCTION

Natural Draft Dry Cooling Towers (NDDCTs) have been successfully used in traditional thermal power plants for several decades. Towers used in such plants are typically more than 100 m in height [1, 2]. Geothermal power plants and concentrated solar thermal (CST) power plants are promising renewable power generation systems. Compared with conventional thermal power plants, these plants are likely to be smaller and usually located in water deficient areas [3]. Short-NDDCTs, which can effectively discharge heat and do not consume any water and electricity, are likely to be a feasible cooling technology for these kinds of power plants [4, 5] . Past studies have identified the vulnerability of short natural draft towers to ambient influences, especially the crosswind and the hot ambient temperature [6-9]. This paper describes the simulated performance of a 20m tall experimental NDDCT constructed at the University of Queensland.

Kroger *et al*. [1] summarized the past researches on air-cooled heat exchangers and the fluids mechanics and proposed a useful 1-D analytical model to predict the cooling efficiency of NDDCTs in the absence of crosswind. Their 1-D model combines the energy balance equations and the air flow draft equations and have been validated against the industrial data [1]. When these two groups of equations are both satisfied, the cooling performance of the NDDCT can be calculated.

The influence of the crosswind has received significant attention in the last few decades[10-12]. Su *et.al* [13] simulated the fluid flow and the temperature distribution of the

dry cooling tower under the crosswind. The results without crosswind have been compared against those obtained with crosswind, at the speeds of 5 and 10 m/s. Based on the simulation result, the authors explained how the crosswind affects the cooling performance of the tower. Al-Waked and Benhia [6] analysed the performance of a NDDCT under crosswind using a three-dimensional computational model. The effectiveness of the windbreak walls has also been studied in this paper. The authors proposed the ratio of the amount heat at crosswind condition to the maximum amount of rejected heat which occurs in the windless condition to better express the effect of the crosswind. According to their simulation results, the crosswind velocity has a big effect on the cooling performance of the NDDCT. The cooling performance drops by 30% when the wind velocity exceeds 10 $m.s^{-1}$. Lu *et.al* [14, 15] investigated the crosswind effect on small sized NDDCTs. They examined the simulated performance of a 15 m NDDCT with horizontally-arranged heat exchangers. Different velocities and different angles of the wind were discussed. Zhao *et al* [16, 17] studied the cooling performance of a NDDCT with vertical delta radiators under the constant heat load. With constant heat load and uniform water inlet temperature, the cooling performance of each heat exchanger sector was analysed under crosswind impact. The authors claimed that with increasing crosswind velocity, the cooling performance of NDDCT under constant heat load deteriorates sharply at low velocity, but varies slightly at high velocity.

QGECE has been developing the small size NDDCT for CST and geothermal power generation systems [8, 14, 15, 18]. This research is necessary because the existing NDDCT design is optimised for large stream power plant, and is not optimal for a CST plant. A 20m high NDDCT designed for CST power plant is commissioned and will be tested for the future application as a part of CST energy system. Based on the above literature review, for short NDDCTs (less than 30m height), their cooling performance is more sensitive to the ambient conditions. Therefore, an accurate simulation of the ambient influence on a small sized NDDCT is a very important prerequisite for the future test on the same NDDCT. In this paper, the results of the 1-D and 3-D models of the Gatton NDDCT are presented. The objectives of this work are as follows: (1) to study the influence of the ambient temperature and crosswind on this specific small NDDCT. (2) to prepare the future test on the same NDDCT.

2. 1-D SIMULATIONS

The simulated cooling tower is of hyperbolic shape and is 20m high with the base diameter of 12 m. Fig. 1 presents the configuration of the tower. The 18 heat exchanger bundles are located horizontally above the inlet cross section of the tower.

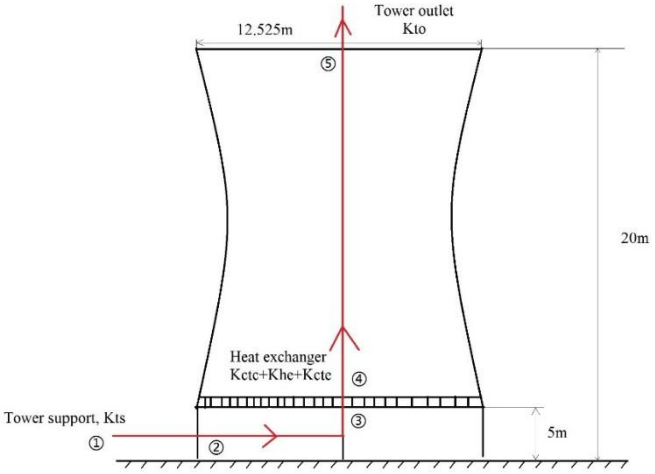

Figure 1: Gatton cooling tower configuration

To calculate the performance of the cooling tower, the energy balance equations and draft equations must be satisfied simultaneously. The assumptions of the 1D model are as following: 1) The cooling tower is operated in the stable condition. 2). The flow resistances other than tower support, the heat exchanger and the tower outlet were neglected. 3) The heat transfer process only happens in the air-cooled heat exchanger. As presented in Fig. 1, the pressure drops between positions 1 and 5 include: the tower support resistance (K_{ts}), the heat exchanger compact resistance (K_{ctc}), the heat exchanger expansion resistance (K_{cte}), the heat exchanger bundle resistance (K_{he}) and the tower outlet resistance (K_{to}).

Using these five coefficients, the draft equation of the cooling tower can be expressed as [1]

$$p_{a1}\left\{\left[1-\frac{0.00975(H_3+H_4)}{2T_{a1}}\right]^{3.5}\times\left[1-\frac{0.00975\left(H_5-\frac{H_3}{2}-\frac{H_4}{2}\right)}{T_{a4}}\right]^{3.5}-\left(\frac{1-0.00975H_5}{T_{a1}}\right)^{3.5}\right\}$$
$$=\frac{(K_{ts}+K_{ctc}+K_{he}+K_{cte})\left(\frac{m_a}{A_{fr}}\right)^2}{2\rho_{a34}}\times\left[1-\frac{0.00975\left(H_5-\frac{H_3}{2}-\frac{H_4}{2}\right)}{T_{a4}}\right]^{3.5}$$
$$+\frac{(1+K_{to})\left(\frac{m_a}{A_5}\right)^2}{2\rho_{a5}} \tag{1}$$

The definitions of all terms can be found in the Nomenclature table. The tower support loss coefficient based on the conditions at the tower support is given by Kroge [1]

$$K_{ts}=C_{Dts}L_{ts}d_{ts}n_{ts}/\pi d_3H_3 \tag{2}$$

The heat exchanger contraction and expansion loss coefficients can be calculated using the Eqs. (3) and (4) respectively [1].

$$K_{ctc}=1-\frac{2}{\sigma_c}+\frac{1}{\sigma_c^2} \tag{3}$$

$$K_{cte}=\left(1-\frac{A_{e3}}{A_3}\right)^2 \tag{4}$$

For towers with cylindrical outlets, the loss coefficient is given by [1]

$$K_{to}=-0.28Fr_D^{-1}+0.04Fr_D^{-1.5} \tag{5}$$

where

$$Fr_D^{-1}=\left(\frac{m_a}{A_5}\right)^2/[p_{a5}(\rho_{a5}-\rho_{a6})gd_5] \tag{6}$$

The logarithmic mean temperature difference method was selected to calculate heat transfer process of the heat exchanger [19]. The heat transferred in the air-cooled heat exchanger can be presented by Eqs. (7) or (8).

$$Q = UA\frac{(T_{\mathrm{wi}} - T_{\mathrm{ao}}) - (T_{\mathrm{wo}} - T_{\mathrm{ai}})}{\ln\left[\frac{(T_{\mathrm{wi}} - T_{\mathrm{ao}})}{(T_{\mathrm{wo}} - T_{\mathrm{ai}})}\right]} \tag{7}$$

or

$$Q = m_{\mathrm{a}}c_{\mathrm{pa}}(T_{\mathrm{ao}} - T_{\mathrm{ai}}) = m_{\mathrm{w}}c_{\mathrm{pw}}(T_{\mathrm{wi}} - T_{\mathrm{wo}}) \tag{8}$$

For NDDCTs, the air-cooled heat exchanger is one of the most important part and in an air-cooled heat exchanger, the air side loss contributes the most heat transfer resistance [19]. To simplify the calculation, this paper correlated the heat transfer coefficient (UA) and the loss coefficient (K_{he}) as functions of Reynold number of the air (Re_{air}). The software Aspen Exchanger Design and Rating was used to get the correlations of Re_{air} with UA and K_{he}. The simulation results have been compared with the data provided by the heat exchanger manufacturer. The deviation of the simulation is less than 3%.

For this particular heat exchanger configuration in the Gatton cooling tower, Eq. (9) and (10) express the correlations of Re_{air} and UA and K_{he}., respectively,

$$UA = -0.0422Re_{\mathrm{air}}^2 + 166.6Re_{\mathrm{air}} + 27226 \tag{9}$$

$$K_{\mathrm{he}} = 0.00005Re_{\mathrm{air}}^2 - 0.0743Re_{\mathrm{air}} + 58.889 \tag{10}$$

Based on Eqs. (1) to (10), the 1-D model of the NDDCT can be built and a solution can be obtained through a simple iterative procedure. Fig.2 is the flow chart of the iteration process, which is described as the following:

1) Input the tower configuration parameters, the heat exchanger parameter, the water input conditions and the ambient conditions;
2) Assume the outlet temperature of the heat exchanger T_{a4} equal to the water inlet temperature T_{wi};
3) Calculate the air mass flow rate m_{a} using the draft equations: Eqs. (1) to (6) and (10);
4) Use the energy balance equation: Eq. (8) to get the outlet temperature of the water and the air enthalpy change Q_1;
5) Use heat exchanger equation Eqs. (7) and (9) to get the heat flux of the air-cooled heat exchanger Q_2;
6) Take n as 10^4, if $|Q_1\text{-}Q_2| > n$, set $T_{\mathrm{a4}}=T_{\mathrm{a4}}\text{-}T_{\mathrm{step}}$, then repeat steps 3 to 5;
7) Output the results when $|Q_1\text{-}Q_2| < n$;

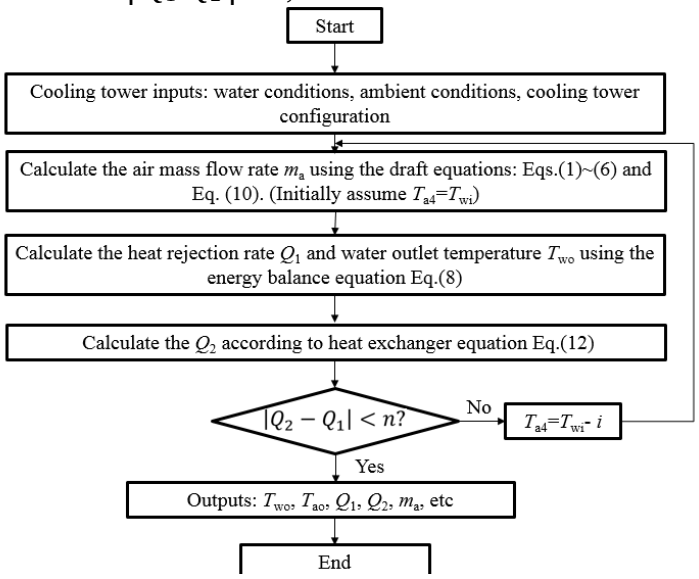

Figure 2: Flow chart of the iteration process of the 1D model

3. 3-D CFD MODELLING

A one-dimensional model is not capable to simulate the crosswind effect. To investigate the crosswind effect on the cooling tower performance, this study used ANSYS Fluent to build a 3-D CFD model of the Gatton cooling tower. The cooling performance under different crosswind conditions was modelled.

3.1 Mesh and geometry

The geometry of the cooling tower in this CFD model is the same as the physical size of the Gatton cooling tower. In this simulation, the cooling tower has been divided into 3 parts: the tower support, the heat exchanger and the main tower. In order to get an accurate result and better compare with the future experiment, the geometry of the heat exchanger is set as same with the experimental cooling tower. So that the single heat exchanger performance can be calculated and compared with experimental result later. A 90 m high cylinder with a diameter of 144 m is set as the computational domain area. Fig. 3 shows the geometry of the 3-D model.

About 1, 320, 000 unstructured prism cells are used in the model. The grid-independence test has been done. The deviation of the results was less than 1% when the quantity of the cells is over 1, 300, 000. The ANSYS meshing high smoothing and slow transition curvature size function are adopted to generate the mesh. The element size of the tower and heat exchanger is set to be 0.3m while the element size of the computation domain area is 0.5 m.

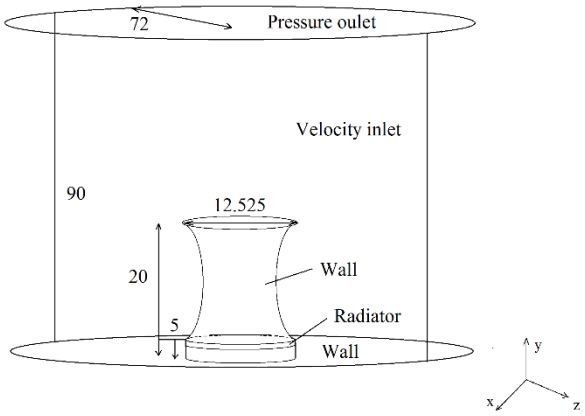

Figure 3: Geometry diagram of the 3-D model

3.2 Boundary condition

The bottom face of the computation domain and tower surface are defined as the zero heat flux and non-slip wall with the standard wall function. In windless condition, the side face of the cylinder is defined as the pressure inlet boundary and the pressure outlet boundary condition is applied on the top face of the cylinder. In the crosswind condition, a velocity inlet boundary condition is applied at the side face of the cylinder, with the velocity profile define as:

$$\frac{v_{cw}}{v_{ref}} = \left(\frac{y}{y_{ref}}\right)^{0.2} \quad (11)$$

The temperatures and pressures at both the inlet and outlet boundaries are set same as the ambient one. Because of the low-turbulence level of advection natural wind, the impact of the turbulence intensity and viscosity ratio was very little at the computation domain boundaries [24]. They can be set as 0.1% and 0.1, respectively.

The heat exchanger bundles in the cooling tower are modelled by the radiator model with a porous zone. The internal structure of the air cooled heat exchangers are simplified as a porous media zone which represents all the air flow resistances within the heat exchangers. According to FLUENT user's guide, the heat transfer process in the radiator can be expressed by Eq. (12).

$$q = \frac{\dot{m} c_p \Delta T}{A} = h(T_{\mathrm{r}} - T_{\mathrm{ao}}) \tag{12}$$

The pressure drop of the system heat exchanger bundles is modelled by porous zone through adding a momentum source term into the corresponding momentum equation. As presented in Eq. (13), the source term is composed by two parts: a viscous loss term and an inertial loss term.

$$S_i = -\left(\frac{\mu}{\alpha} v_i + C_2 \frac{1}{2} \rho |v| v_j\right) \tag{13}$$

The parameters in Eqs (12) and (13) can be correlated by calculating the 1-D model under different conditions.

3.3 Governing Equations

According to the previous research [16-18, 20-23], the realizable *k-ε* model has been selected in this study. The general term of the governing equations can be expressed as:

$$\nabla.\left(\rho u \phi - \Gamma_\phi \nabla \phi\right) = S_\phi \tag{14}$$

Table. 1 presented the expression of the three parameters in the above equation.

Table 1: The 3-D governing equation parameter from Eq. (14)

	ϕ	S_ϕ	Γ_ϕ
Continuity	1	0	0
x momentum	U	$-\frac{\partial p}{\partial x} + \frac{\partial}{\partial x}\left(\mu_e \frac{\partial U}{\partial x}\right) + \frac{\partial}{\partial y}\left(\mu_e \frac{\partial V}{\partial x}\right) + \frac{\partial}{\partial z}\left(\mu_e \frac{\partial W}{\partial x}\right) + \frac{\Delta p_x A_c}{V_c}$	μ_e
y momentum	V	$-\frac{\partial p}{\partial y} + \frac{\partial}{\partial x}\left(\mu_e \frac{\partial U}{\partial y}\right) + \frac{\partial}{\partial y}\left(\mu_e \frac{\partial V}{\partial y}\right) + \frac{\partial}{\partial z}\left(\mu_e \frac{\partial W}{\partial y}\right) + \frac{\Delta p_y A_c}{V_c}$	μ_e
z momentum	W	$-\frac{\partial p}{\partial z} + \frac{\partial}{\partial x}\left(\mu_e \frac{\partial U}{\partial z}\right) + \frac{\partial}{\partial y}\left(\mu_e \frac{\partial V}{\partial z}\right) + \frac{\partial}{\partial z}\left(\mu_e \frac{\partial W}{\partial z}\right) + \frac{\Delta p_z A_c}{V_c}$	μ_e
Energy	T	$\frac{1}{c_p}\left(\frac{q A_c}{V_c}\right)$	$\frac{\mu}{\mathrm{Pr}} + \frac{\mu_t}{\mathrm{Pr}_t}$
Turbulent energy	k	$G_k + G_b - \rho\varepsilon$	$\frac{\mu_e}{\sigma_k}$

Energy dissipation	ε	$C_{1\varepsilon}\frac{\varepsilon}{k}(G_k + C_{3\varepsilon}G_b) - C_{2\varepsilon}\rho\frac{\varepsilon^2}{k}$	$\frac{\mu_e}{\sigma_\varepsilon}$

where

$$G_k = \mu_e\left\{2\left[\left(\frac{\partial U}{\partial x}\right)^2 + \left(\frac{\partial V}{\partial y}\right)^2 + \left(\frac{\partial W}{\partial z}\right)^2\right] + \left(\frac{\partial V}{\partial x} + \frac{\partial U}{\partial y}\right)^2 + \left(\frac{\partial V}{\partial z} + \frac{\partial W}{\partial y}\right)^2 + \left(\frac{\partial U}{\partial z} + \frac{\partial W}{\partial x}\right)^2\right\}$$

$\mu_e = \mu + \mu_t$; $\mu_t = C_\mu \rho \frac{k^2}{\varepsilon}$; $C_{1\varepsilon} = 1.44$; $C_{2\varepsilon} = 1.92$; $C_{3\varepsilon} = \tanh(\frac{U_{pa}}{U_{pe}})$;

$G_b = -g\frac{\mu_t}{\rho \mathrm{Pr}}\frac{\partial \rho}{\partial y}$; $C_\mu = 0.09$; $\sigma_k = 1.0$; $\sigma_{k\varepsilon} = 1.3$; Pr=0.74; Pr_t=0.85

4. RESULTS AND DISCUSSIONS

4.1 1-D simulation result

In the present 1-D simulation, the water mass flow rate is fixed at 14.8 kg.s^{-1}. The temperature of the hot water inlet is ranged from 53.31 ℃ to 83.31 ℃ while the ambient temperature varies from 15 ℃ to 45 ℃. Figs. 4 and 5 presents the variations in the air mass flow rate and the heat rejection rate of the cooling tower.

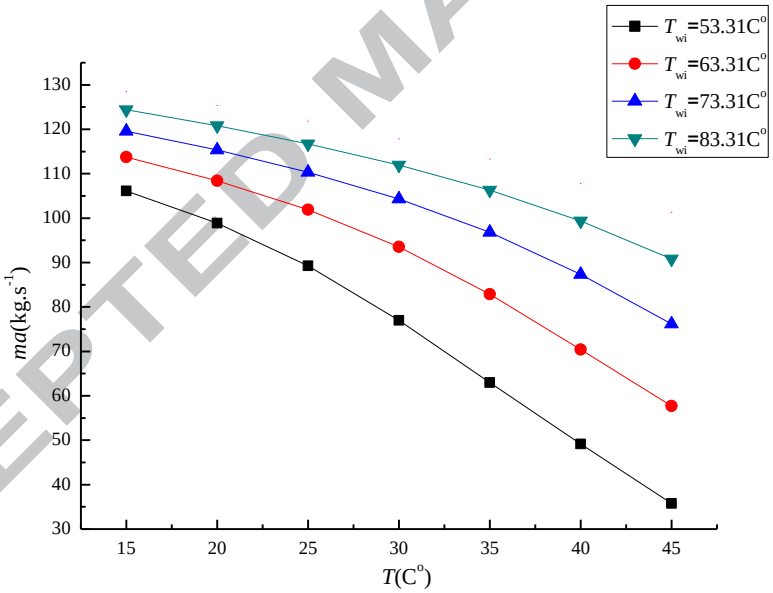

Figure 4 The air mass flow rate of the Gatton NDDCT at different ambient temperature

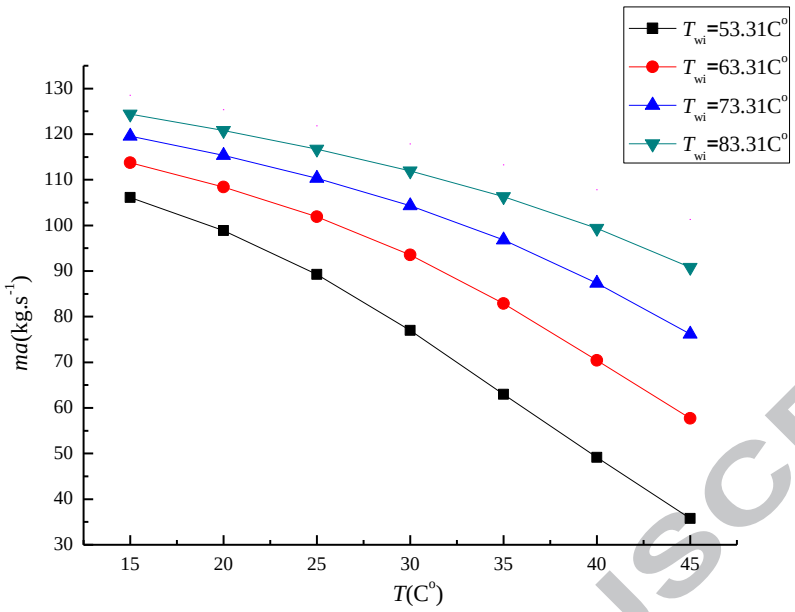

Figure 5 The heat rejection rate of the Gatton NDDCT at different ambient temperature

Figs. 4 and 5 show that, both the heat rejection rate and the air mass flow rate decrease as the ambient temperature increases or the hot water inlet temperature decreases. Within the ambient temperature changes from 15 ℃ to 45 ℃., the air mass flow rate decreases by 66%, 49%, 36% and 27%, when the hot water temperatures are 53.31 ℃, 63.31 ℃ 73.31 ℃ and 83.31 ℃, respectively. These drops in heat rejection are heat rejection rate are 87%, 71%, 58% and 48%, respectively. It can be seen in Figs. 4 and 5, the cooling tower performance is more sensitive when the hot water temperature is close to the ambient temperature.

Eq. (15) is the simplified draft equation of the cooling tower. The right side of the equation presents the draft provided by the cooling tower while the left side is the air flow resistance in the cooling tower. In a NDDCT, the air flow in the cooling tower is mainly determined by the air density difference, the draft height and the pressure loss of the heat exchanger. For a given cooling tower, the main influencing factor of the air flow is the density difference between the hot air inside the tower and the cool air outside the tower.

$$\rho_{a34} v_a^2 K_T/2 = (\rho_{a4} - \rho_{a3})g(H_5 - H_4) \tag{15}$$

Based on the physical property of the air, the larger the temperature difference between hot and cool air, the bigger the air density difference exists. The rise in ambient temperature and the decrease in hot water temperature both decrease the temperature difference between the inside and outside air of the tower. Thus, the air flow rate passing through the tower was adversely influenced. The cooling performance of NDDCTs relies mainly on the convective heat transfer created by the natural draft effect and thus not as effective as that in wet cooling towers. So the cooing performance is particularly reduced when the ambient air is hot.

For the CST plant using the super-critical CO_2 power cycle proposed by the University of Queensland, the condensing temperature is around 70 ℃. When the ambient temperature varies from 15 ℃ to 40 ℃, the heat rejection rate of the cooling tower changes correspondingly from 3.1 MW to 1.9 MW. Considering the higher thermal efficiency of the

supercritical CO_2 cycle and hence the relatively smaller cooling requirement, this small size NDDCT is suitable for the CST power plant with 2~3MW nominal net power.

4.2 3-D simulation result

The cooling performance of Gatton tower was simulated using the 3-D model described in Section 3. The simulation results of the 3-D model were first compared with 1-D model in no crosswind condition. Fig. 6 gives the comparison of the 1-D and 3-D model results in different ambient temperature. The numerical results of the 3D model in no-wind case have a good consistence with the 1-D model. The deviations between the 1-D and 3-D models in air outlet mass flow rate and air outlet temperature are about 1.3% and 1.5% respectively.

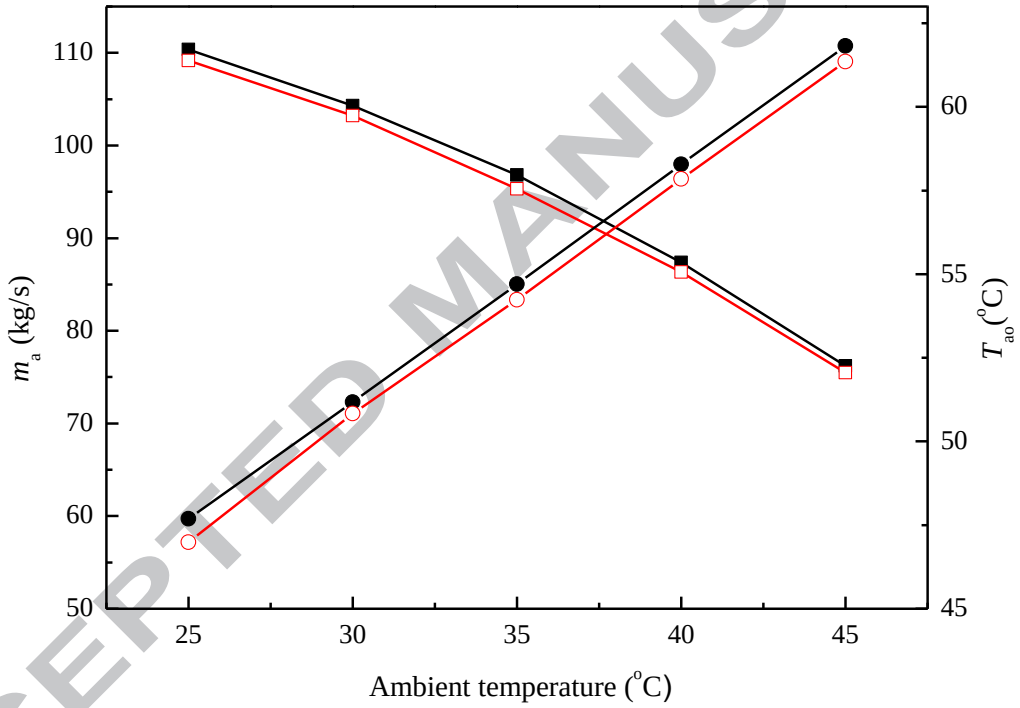

Figure 6 Comparison between the 1-D model and the 3-D model: ■ m_a calculated by 1-D model □ m_a calculated by 1-D model ● T_{ao} calculated by 1-D model ○ T_{ao} calculated by 3-D model

Different crosswind velocities ranging from 0 m/s to 15 m/s are discussed in this paper. The heat exchanger temperature is set to be 50 ℃ and the ambient temperature is 25 ℃ in the simulation. Fig. 7 presents the air stream line of the cooling tower at different crosswind velocities. In the simulation, the crosswind is aligned with z axis direction.

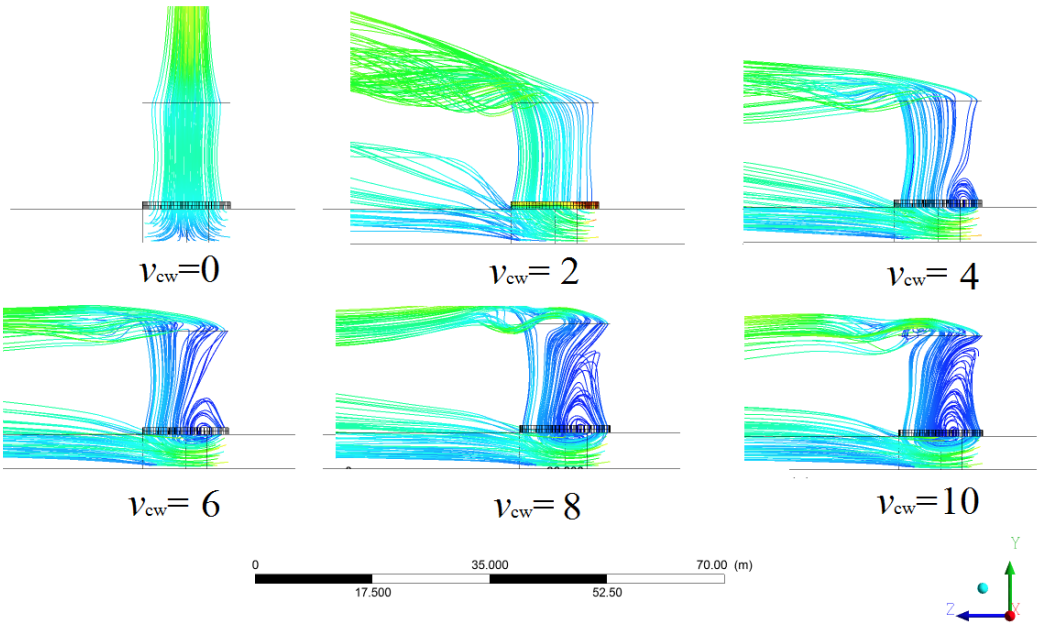

Figure 7: 3-D steam lines of the cooling tower in different crosswind condition

In Fig. 7 the ambient air is moving through the heat exchanger from the tower bottom towards the top driven by the natural draft when there is no crosswind. In such a case, the air flow near the edge of the heat exchanger is slightly smaller than that in the centre. This is because the resistance near edge of the heat exchanger is larger than that in the centre area. When crosswind appears, the air flow inside the tower is disturbed. Under low crosswind speed (less than 4 m/s) condition, the air flow in the windward part of the heat exchanger is decreased and thus smaller than that in the leeward part. Once the speed reaches 4 m/s or above, the vortices are formed in the tower. The vortices at the bottom of the cooling tower redistribute the hot air above the heat exchanger and thus further impair the heat transfer. With the further increase of the crosswind speed, vortices are also generated at the top of the cooling tower which making the air difficult to exit the tower. Consequently, both the air flow process and the heat transfer in the tower are reduced by the crosswind.

Fig. 8 is the pressure profile at the bottom of the cooling tower. With the acceleration of the air as it flows around the lower part of the cooling tower, a low pressure area is generated at the windward part of the cooling tower and the air flow is seriously affected in this area. When crosswind speed is small, this low pressure area decreases the air flow mass flow rate in this area by decreasing the air pressure difference. As the crosswind increases, the pressure distribution is even more un-uniform in windward area, which result in the sucking out of the hot air from the cooling tower. Thus in Fig.7, the vortices are seen in this area when the crosswind speed is large enough.

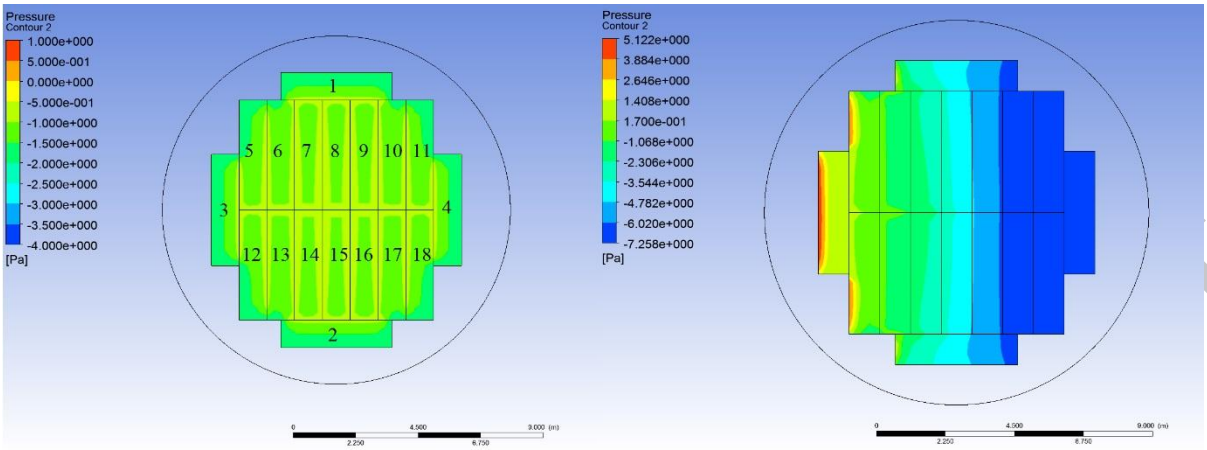

Figure 8 Pressure contour at the bottom of the heat exchanger at crosswind speed of 0 m/s and 4 m/s

Fig. 9 presents the temperature contours at the middle cross section of the tower. With the influence of the crosswind, a high temperature region was formed on the windward side of the cooling tower, due to the decreasing of the amount of cold air in this area. On the other hand, for the cooling towers which have the horizontally placed heat exchanger, the heat can be dumped from both the bottom and the top of the tower [18]. According to the temperature contour, when crosswind exists, the heat from the heat exchanger will be taken away by both the upward air steam created by the buoyance force and the forced convection created by the wind. Thus in Fig. 9, a high temperature area is generated at the bottom of the heat exchanger when the crosswind occurs.

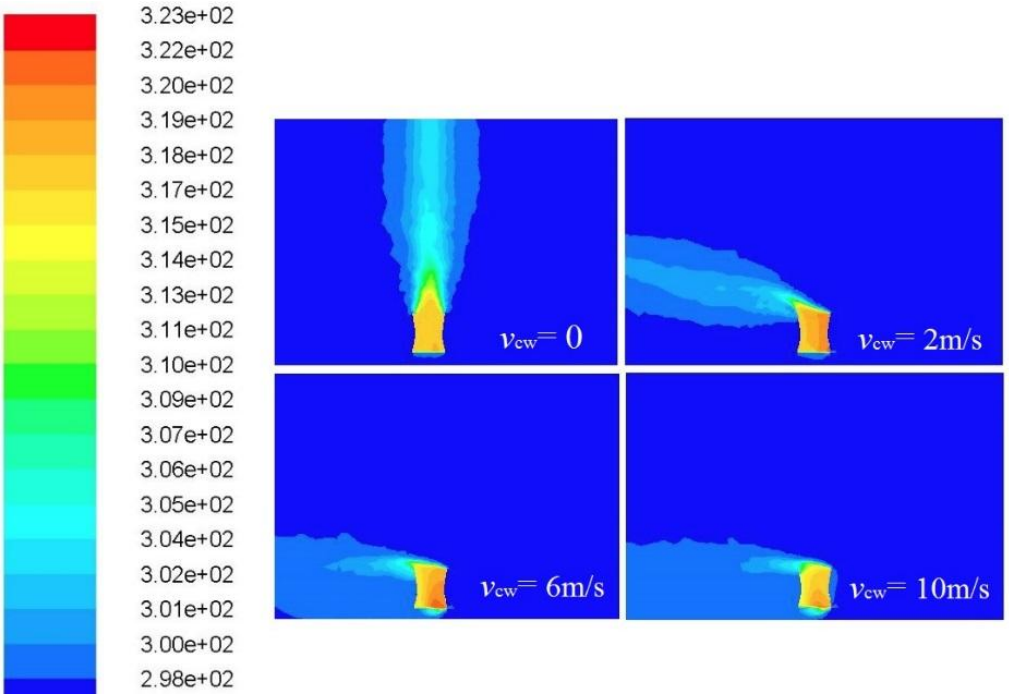

Figure 9: The temperature contour of the tower in different crosswind condition

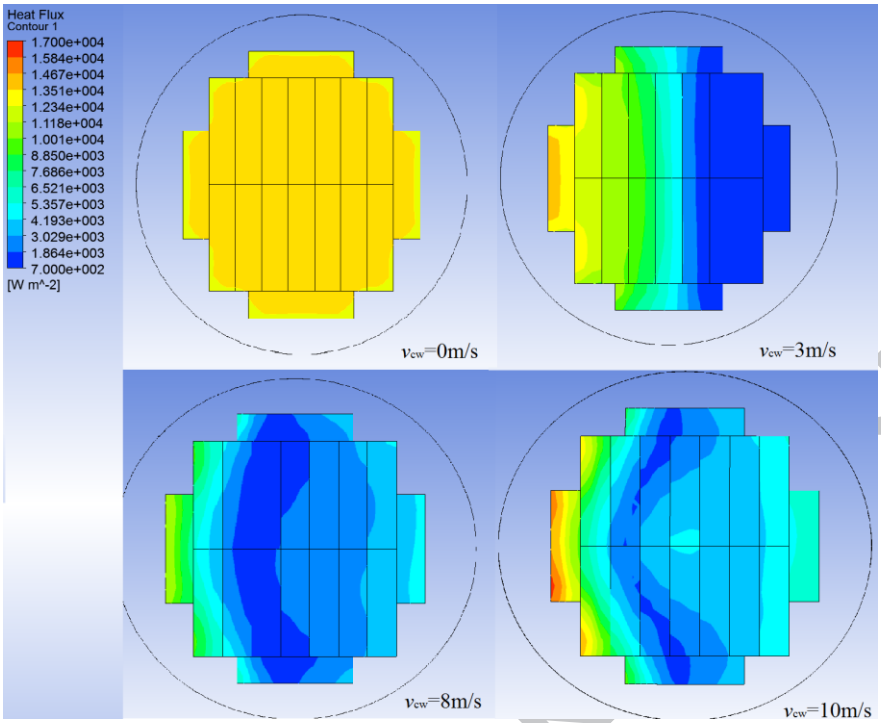

Figure 10 The heat transfer rate of the heat exchanger when crosswind speed is 0 m/s, 3 m/s, 8 m/s and 10 m/s

Fig. 10 shows the heat flux of the 18 heat exchangers at the bottom of the cooling tower under different crosswind conditions. The heat flux in each heat exchanger bundles was almost the same when there is no wind. When the crosswind speed is 3 m/s, the low pressure effect showed in Fig.8 is produced at the windward part of the heat exchanger. This effect decreases the upward air flow thus reduce the cooling performance in this area. However, with the appearance of the crosswind, the force convection occurs at the bottom of the cooling tower. According to previous research [18, 19], the heat transfer coefficient of the force convection of a plane can be calculated by $Nu = aRe_x Pr^{1/3}$, where Re_x is based on the crosswind speed and the length of the heat exchanger. So with the increase of the crosswind speed, the amount of the heat transferred by the force convection increased. So in Fig. 9, the heat exchanger performance at the windward part is improved gradually. The crosswind decreases the buoyance effect by disturbing the air flow and the heat transfer in the tower. But it also increases the force convection at the bottom of the heat exchanger.

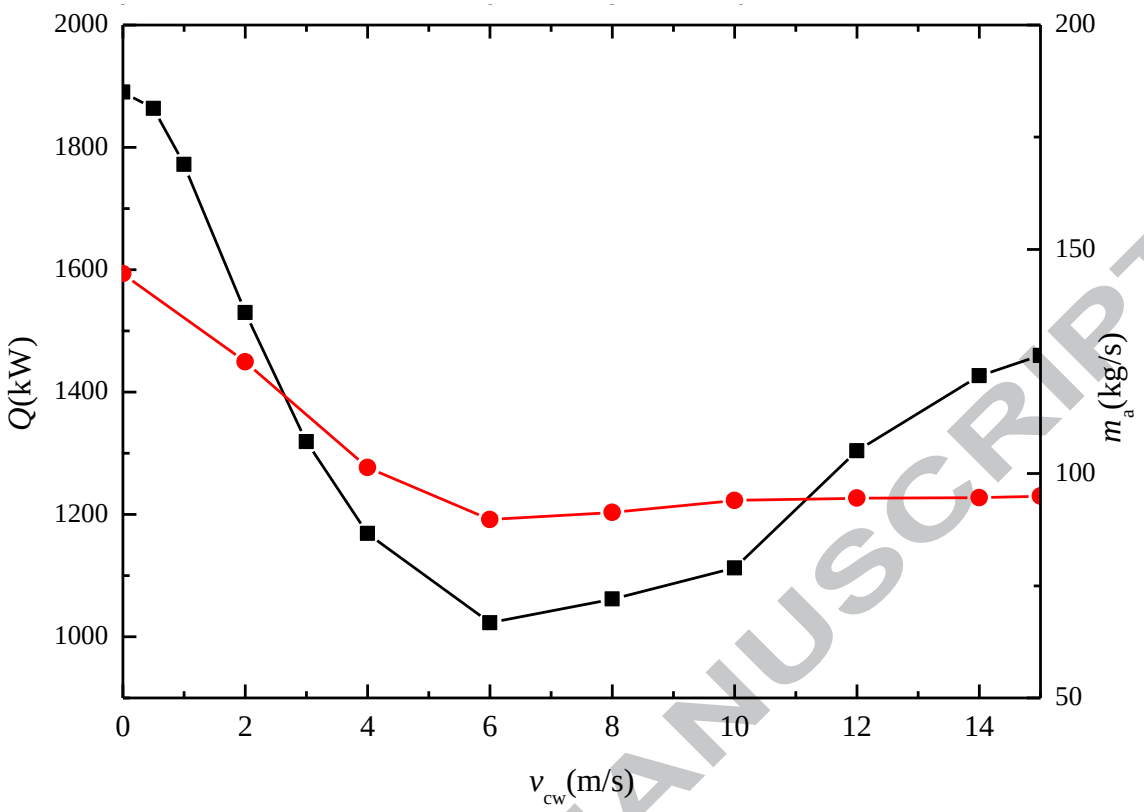

Figure 11 Heat rejection ratio and air mass flow rate at different crosswind condition: ■, heat rejection rate, ●, air mass flow rate

Fig. 11 demonstrates the variation of the air mass flow rate and heat rejection rate under the crosswind speed range from 0 m/s to 15 m/s. When the crosswind increasing from 0 m/s to 6 m/s, the heat rejection rate decreases rapidly with the increase of the crosswind velocity, due to the adversely crosswind effect on the air flow mass flow rate. When v_{cw}=6 m/s, the air mass flow rate reached the minimum as well as the heat rejection rate. Fig. 12 presents the air mass flow rate distribution under crosswind condition of 0 m/s and 6 m/s, the number of each heat exchanger can be found in Fig.8. It can be seen that the air mass flow rate of the heat exchanger bundles located at the windward direction of the cooling tower decrease more than 70% compared with the windless condition. These air-cooled heat exchangers do not function well because of the supply of the cold air is too small. However, when v_{cw} exceed 6 m/s, the air mass flow rate varies little and the heat rejection rate increases with the increase in the crosswind velocity. This is because of the forced convection at the bottom of the heat exchangers. It can be expected from the curve that if the crosswind speed is sufficiently high, the total heat dumping rate of the cooling tower will recover to the level in non-wind case. However, the crosswind is still a negative factor on the cooling performance since the natural draft effect is the main source to dump the heat in a NDDCT.

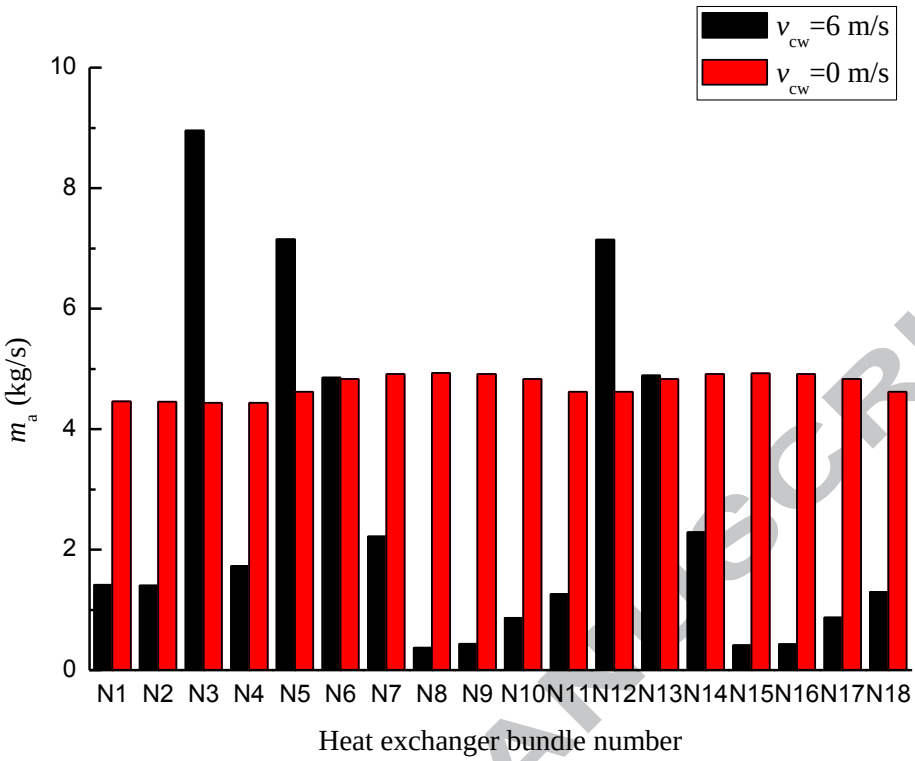

Figure 12 Air mass flow rate of each heat exchanger bundle when crosswind is 0 m/s and 6 m/s

The above simulation results provide technical data and guidelines to the future experimental work. The simulations predict the possible air and water temperature ranges during the operation of the full scale experimental cooling tower. The ranges help to select proper instrumentations and refine the testing procedure, so that the experiment cost can be minimized. On the other hand, the planed future experiment work will be used to validate the simulation results. The performance of the cooling tower will first test at the windless condition and in different ambient temperature under which the 1-D model simulation was carried out. Then the crosswind affect will be considered, the 3D CFD results of the temperature distribution and air velocity distribution in the cooling tower and the thermal performance of each heat exchanger bundle will be compared to the measurement.

5. CONCLUSIONS

The full scale 1-D and 3-D model of the Gatton NDDCT has been established. The influence of hot water inlet temperatures, ambient temperatures and crosswind velocities on the cooling performance a 20m NDDCT was analysed and discussed in this paper. The current study draws the following conclusions:

1. Under non-crosswind condition, the heat rejection rate of the current cooling tower is able to reject about 1.9MW to 3.1MW at the inlet water temperature of 70℃ when the ambient temperature ranges in 15℃ to 35℃. This tower is promising for a 2~3MW CST plant using supercritical CO_2 cycle proposed by the University of Queensland.

2. Both the inlet water temperature and the ambient temperature have significant influence on the cooling performance of the NDDCT. These two factors influence the tower performance through decrease the driving force of the air flow and heat transfer process.

3. The heat can be dumped from both the bottom and the top in a short NDDCT when the crosswind exists. The crosswind decreases the buoyance effect by disturbing the air flow and the heat transfer in the tower, but it causes the forced convection at the bottom of the tower as well.

ACKNOWLEDGEMENTS

This research was performed as part of the Australian Solar Thermal Research Initiative (ASTRI), a project supported by Australian Government. The author, Xiaoxiao Li, would also like to thank China Scholarship Council (CSC) for their financial support.

REFERENCES

[1] D.G. Kröger, Air-cooled heat exchangers and cooling towers, Pennwell Corp, Tulsa, Oklahoma, 2004.
[2] G.B. Hill, E.J. Pring, P.D. Osborn, Cooling towers: principles and practice, third ed., Butterworth-Heinemann, London, 1990.
[3] B.K. Hodge, Alternative energy systems and applications, Wiley, Hoboken, 2010.
[4] H. Gurgenci, Z. Guan, Dirigible natural draft cooling tower in geothermal and solar power plant applications, in: Proceedings of 14th IAHR International Conference on Cooling Tower and Air-Cooled Heat Exchangers, Stellenbosch, 2009.
[5] K. Hooman, Dry cooling towers as condensers for geothermal power plants, Int. Commun. Heat Mass Transfer, 37 (2010) 1215-1220.
[6] R. Al-Waked, M. Behnia, The performance of natural draft dry cooling towers under crosswind: CFD study, Int. J. Energy Res., 28 (2004) 147-161.
[7] S. He, H. Gurgenci, Z. Guan, X. Huang, M. Lucas, A review of wetted media with potential application in the pre-cooling of natural draft dry cooling towers, Renewable Sustainable Energy Rev., 44 (2015) 407-422.
[8] Y. Lu, Small natural draft dry cooling towers for renewable power plants, PhD Thesis, The University of Queensland, School of Mechanical and Mining Engineering, 2015.
[9] H. Ma, F. Si, L. Li, W. Yan, K. Zhu, Effects of ambient temperature and crosswind on thermo-flow performance of the tower under energy balance of the indirect dry cooling system, Appl. Therm. Eng., 78 (2015) 90-100.
[10] A.F. du Preez, D.G. Kröger, The effect of the heat exchanger arrangement and wind-break walls on the performance of natural draft dry-cooling towers subjected to cross-winds, J. Wind Eng. Ind. Aerodyn., 58 (1995) 293-303.
[11] Q. Wei, B. Zhang, K. Liu, X. Du, X. Meng, A study of the unfavorable effects of wind on the cooling efficiency of dry cooling towers, J. Wind Eng. Ind. Aerodyn., 54–55 (1995) 633-643.
[12] T.J. Bender, D.J. Bergstrom, K.S. Rezkallah, A study on the effects of wind on the air intake flow rate of a cooling tower: Part 3. Numerical study, J. Wind Eng. Ind. Aerodyn., 64 (1996) 73-88.
[13] M.D. Su, G.F. Tang, S. Fu, Numerical simulation of fluid flow and thermal performance of a dry-cooling tower under cross wind condition, J. Wind Eng. Ind. Aerodyn., 79 (1999) 289-306.
[14] Y. Lu, Z. Guan, H. Gurgenci, Z. Zou, Windbreak walls reverse the negative effect of crosswind in short natural draft dry cooling towers into a performance enhancement, Int. J. Heat Mass Transfer, 63 (2013) 162-170.

[15] Y. Lu, H. Gurgenci, Z. Guan, S. He, The influence of windbreak wall orientation on the cooling performance of small natural draft dry cooling towers, Int. J. Heat Mass Transfer, 79 (2014) 1059-1069.
[16] Y. Zhao, G. Long, F. Sun, Y. Li, C. Zhang, J. Liu, Effect mechanism of air deflectors on the cooling performance of dry cooling tower with vertical delta radiators under crosswind, Energy Convers. Manage., 93 (2015) 321-331.
[17] Y.B. Zhao, G. Long, F. Sun, Y. Li, C. Zhang, Numerical study on the cooling performance of dry cooling tower with vertical two-pass column radiators under crosswind, Appl. Therm. Eng., 75 (2015) 1106-1117.
[18] Y. Lu, Z. Guan, H. Gurgenci, K. Hooman, S. He, D. Bharathan, Experimental study of crosswind effects on the performance of small cylindrical natural draft dry cooling towers, Energy Convers. Manage., 91 (2015) 238-248.
[19] Y.A. Çengel, A.J. Ghajar, Heat and mass transfer: fundamentals & applications, McGraw-Hill, New York, 2015.
[20] R. Al-Waked, Crosswinds effect on the performance of natural draft wet cooling towers, Int. J. Therm. Sci., 49 (2010) 218-224.
[21] Z. Zou, Z. Guan, H. Gurgenci, Y. Lu, Solar enhanced natural draft dry cooling tower for geothermal power applications, Sol. Energy, 86 (2012) 2686-2694.
[22] L.J. Yang, L. Chen, X.Z. Du, Y.P. Yang, Effects of ambient winds on the thermo-flow performances of indirect dry cooling system in a power plant, Int. J. Therm. Sci., 64 (2013) 178-187.
[23] L.J. Yang, X.P. Wu, X.Z. Du, Y.P. Yang, Dimensional characteristics of wind effects on the performance of indirect dry cooling system with vertically arranged heat exchanger bundles, Int. J. Heat Mass Transfer, 67 (2013) 853-866.
[24] Y. Zhao, F. Sun, Y. Li, G. Long, Z. Yang, Numerical study on the cooling performance of natural draft dry cooling tower with vertical delta radiators under constant heat load, Appl. Energy, 149 (2015) 225-237.